HHS Public Access

Author manuscript

Nat Nanotechnol. Author manuscript; available in PMC 2016 June 21.

Published in final edited form as:

Nat Nanotechnol. 2016 March ; 11(3): 295–303. doi:10.1038/nnano.2015.292.

In situ vaccination with cowpea mosaic virus nanoparticles suppresses metastatic cancer

P. H. Lizotte[1], **A. M. Wen**[4], **M. R. Sheen**[1], **J. Fields**[1], **P. Rojanasopondist**[1], **N. F. Steinmetz**[4,5,6,7,*], and **S. Fiering**[1,2,3,*]

[1]Department of Microbiology and Immunology, The Geisel School of Medicine at Dartmouth, Lebanon, NH 03756

[2]Department of Genetics, The Geisel School of Medicine at Dartmouth, Lebanon, NH 03756

[3]Norris Cotton Cancer Center, Lebanon, NH 03756

[4]Department of Biomedical Engineering, Case Western Reserve University Schools of Engineering and Medicine, Cleveland, OH 44106

[5]Department of Radiology, Case Western Reserve University Schools of Engineering and Medicine, Cleveland, OH 44106

[6]Department of Materials Science and Engineering, Case Western Reserve University Schools of Engineering and Medicine, Cleveland, OH 44106

[7]Department of Macromolecular Science and Engineering, Case Western Reserve University Schools of Engineering and Medicine, Cleveland, OH 44106

Abstract

Nanotechnology has tremendous potential to contribute to cancer immunotherapy. The "*in situ* vaccination" immunotherapy strategy directly manipulates identified tumours to overcome local tumour-mediated immunosuppression and subsequently stimulates systemic anti-tumour immunity to treat metastases. We show that inhalation of self-assembling virus-like nanoparticles from Cowpea Mosaic Virus (CPMV) reduces established B16F10 lung melanoma and simultaneously generates potent systemic anti-tumour immunity against poorly immunogenic B16F10 in the skin. Full efficacy required Il-12, Ifn-γ, adaptive immunity, and neutrophils. Inhaled CPMV nanoparticles were rapidly taken up by and activated neutrophils in the tumour microenvironment

*Co-corresponding authors: Steven Fiering, Ph.D., 622 Rubin, 1 Medical Center Drive, Lebanon, NH 03756. Phone: 603-653- 9966. Fax: 603-653-9952. ; Email: fiering@dartmouth.edu. Nicole F. Steinmetz, Ph.D., Wearn 352, 10990 Euclid Avenue, Cleveland, OH 44106. Phone: 216-844-8165. ; Email: nfs11@case.edu

Author contributions

P.H.L., N.F.S., and S.F. conceived and designed the experiments, and wrote the manuscript. P.H.L., A.M.W., P.R., M.R.S., and J.F. performed the experiments. M.R.S. was responsible for Supplementary Figure 4. P.R. was responsible for Supplementary Figure 6. A.M.W. was responsible for Supplementary Figure 8. P.H.L. performed all other experiments and analysed the data. J.F. assisted with *in vivo* work. All authors commented on the manuscript.

Competing interests

P.H.L., A.M.W., N.F.S., and S.F. have applied for patent protection for the immunotherapeutic use of eCPMV.

Supplementary information accompanies this paper at www.nature.com/naturenanotechnology.

as an important part of the anti-tumour immune response. CPMV also exhibited clear treatment efficacy and systemic anti-tumour immunity in ovarian, colon, and breast tumour models in multiple anatomic locations. CPMV nanoparticles are stable, nontoxic, modifiable with drugs and antigens, and their nanomanufacture is highly scalable. These properties, combined with their inherent immunogenicity and demonstrated efficacy against a poorly immunogenic tumour, make CPMV an attractive and novel immunotherapy against metastatic cancer.

Tumour immunotherapy offers new options for treating metastatic cancer. Novel therapeutics that induce anti-tumour immunity such as immune checkpoint inhibitors[1], chimeric antigen receptor cell therapies[2], and tumour-associated antigen cancer vaccines[3] show considerable progress but the development of immunotherapy for cancer is in an early stage and it is clear that, as with other cancer therapies, immunotherapies will likely be combined for optimal efficacy. Combinations of checkpoint blocking antibodies have additive effects clinically[4] and have demonstrated synergy with immune agonists [5] and conventional chemotherapy[6].

An option with limited recent exploration is direct application of immunostimulatory reagents into the suspected metastatic site or into an identified tumour. This approach, *in situ* vaccination, modulates the local microenvironment to relieve immunosuppression and potentiate anti-tumour immunity against antigens expressed by the tumour. Oncolytic virus[7] and STING agonist[8] are being tested in clinical trials as *in situ* vaccination adjuvants against metastatic melanoma. The response induced by such treatment modalities can lead to systemic anti-tumour immune responses against unrecognised metastases and, since the treatments are local, the side effects are reduced.

Immunotherapy with nanoparticles is a minimally explored area with significant promise for oncology. Research into nanoparticles as cancer therapies has largely focused on them as a delivery platform for conventional chemotherapeutics[9]. However, the tendency of nanoparticles to interact with and to be ingested by innate immune cells gives them potential as immunostimulatory agents that modulate the characteristics of the ingesting innate immune population.

VLPs refer to the spontaneous organisation of viral coat proteins into the three dimensional structure of a particular virus capsid. VLPs are in the 20–500nm size range, but lack virus nucleic acid, so are non-infectious. VLPs are deployed as antigen components of anti-viral vaccines against a variety of infectious counterpart viruses including cancer-causing hepatitis B[10] and human papilloma virus and work via generation of neutralising antibodies against viral coat proteins[11].

Recent studies have demonstrated that some VLPs possess inherent immunogenic properties that stimulate immune responses against pulmonary infectious agents lacking any antigenic relationship to the VLP[12]. These include methicillin-resistant *Staphylococcus aureus* (MRSA)[13], *Coxiella burnetii*[14], and influenza[14–16]. Protective immunity in these models was associated with leukocyte recruitment, activation, and increased antigen-processing capabilities[13,14], formation of inducible bronchus-associated lymphoid tissue[14], and stimulation of $CD4^+$ T and B lymphocytes[14] and $CD8^+$ T cells[15]. The mechanistic basis of

immunomodulation by any VLP is not known, but it is likely that some VLPs have more of that capacity than others.

We sought to investigate whether VLPs could be utilised for treating cancer. Cowpea mosaic virus (CPMV) self-assembles into 30nm icosahedral structures. It consists of 60 copies each of small and large coat protein units[17]. CPMV is a plant virus that can be produced through molecular farming in plants. The particle used in this study is the empty CPMV (eCPMV) VLP system, which does not carry any nucleic acids and is non-infectious. *In planta* production avoids endotoxin contamination that may be a byproduct of VLPs generated in *E. coli*. eCPMV is stable and can be modified to deliver cargo such as drugs or antigens in its hollow core or covalently linked to its coat proteins, and its production is scalable[18,19]. We have investigated the efficacy of the eCPMV nanoparticle as an immunotherapy in models of metastatic lung melanoma and other cancers and found it has striking efficacy in mouse models as an *in situ* vaccination reagent.

eCPMV nanoparticles are immunogenic and suppress lung tumours

For our proposed use of eCPMV as a novel immunotherapy, we first sought to determine its inherent immunogenicity. eCPMV VLPs, lacking any known immunostimulatory component, were added to *in vitro* cultures of bone marrow-derived dendritic cells (BMDCs) and primary macrophages harvested from C57BL6 mice. Twenty-four hours of culture with eCPMV particles induced both BMDCs (Fig. 1a) and macrophages (Fig. 1b) to secrete higher levels of canonical pro-inflammatory cytokines including Il-1β, Il-6, Il-12p40, Ccl3 (MIP1-α), and Tnf-α, leading us to conclude that eCPMV is inherently immunostimulatory.

We next determined the immunomodulatory effect of eCPMV inhalation on the lung microenvironment, both in terms of immune cell composition and changes in cytokine and chemokine levels. Exposure of non-tumour-bearing mouse lungs to eCPMV revealed significant activation of $Ly6G^+$ neutrophils 24 hours after exposure as assessed by their upregulation of the CD11b activation marker[20] (Fig. 2a top 2 panels labeled “no tumour” and Supplementary Fig. 1) and CD86 co-stimulatory marker (Supplementary Fig. 2). Interior Alexa488-labeling of the particle allowed for cell tracking without changing the exterior structure of the eCPMV (10), which enabled us to confirm that it is this $CD11b^+Ly6G^+$ activated neutrophil subset, specifically, that takes up the eCPMV (Supplementary Fig. 2).

Lungs of mice bearing B16F10 melanoma tumours revealed a more complex immune cell composition. By day 7 we were able to observe the emergence of large populations of immunosuppressive $CD11b^+Ly6G^-F4/80^{lo}$class-II^-SSC^{lo} monocytic myeloid-derived suppressor cells (MDSCs) and $CD11b^+Ly6G^+F4/80^-$class-$II^{mid}SSC^{hi}$ granulocytic MDSCs (Fig. 2a bottom panels and Supplementary Fig. 3)[21]. We also observed the presence of a small population of $CD11b^{hi}Ly6G^{hi}$class-$II^{mid}CD86^{hi}$ cells that have been described in the literature as “tumour-infiltrating neutrophils” or “N1 neutrophils.” These cells are known to exert an anti-tumour effect through coordination of adaptive immune responses, production of pro-inflammatory cytokines, recruitment of T and NK cells, and direct cytotoxicity to tumour cells[22,23]. Inhalation of eCPMV into B16F10-bearing lungs dramatically altered the

immune cell composition 24 hours after administration. We observed significant increases in the tumour-infiltrating neutrophil (TIN) and $CD11b^{+}Ly6G^{+}$ activated neutrophils populations, as well as a reduction in $CD11b^{-}Ly6G^{+}$ quiescent neutrophils (Fig. 2a bottom panels, see arrows). TIN and activated $CD11b^{+}$ neutrophil populations increased dramatically both as a percentage of $CD45^{+}$ cells and also in total number (Fig. 2b). Interestingly, it is these neutrophil subpopulations that took up the vast majority of eCPMV particles, particularly TINs that took up 10-fold more eCPMV than $CD11b^{+}$ activated neutrophils (Fig. 2c). Monocytic MDSC, quiescent neutrophil, and alveolar macrophage populations did not take up eCPMV, and granulocytic MDSCs displayed uneven uptake. The TIN and activated neutrophil populations also expressed MHC class-II and the TINs, in particular, displayed high levels of co-stimulatory marker CD86, indicating potential antigen presentation and T cell priming capability.

Activation of neutrophil populations by eCPMV is consistent with data collected from a multiplexed cytokine/chemokine array performed on whole lung homogenate of B16F10 tumour-bearing lungs treated with eCPMV or PBS (Fig. 2d). Specifically, we saw significant increases in neutrophil chemoattractants GM-CSF, Cxcl1, Ccl5, and MIP-1α[22] and significant increases in cytokines and chemokines known to be produced by activated neutrophils such as GM-CSF, Il-1β, Il-9, Cxcl1, Cxcl9, Cxcl10, Ccl2, MIP-1α, and MIP-1β[23]. Interestingly, we observed no or modest increases in levels of Il-6 and Tnf-α, classical pro-inflammatory cytokines which may be detrimental in the context of lung immunobiology. The lack of acute lung injury was confirmed by histology of eCPMV- and PBS-treated lungs 24hr after intubation. Immune cell infiltration and the degree of alveolar wall thickening were slightly more pronounced in eCPMV-treated lungs compared to PBS-treated, but the difference was not statistically significant. There was also no difference in lung weight. Moreover, we did not observe any toxicity to other major organs including liver, kidney, heart, and spleen (Supplementary Fig. 4).

We determined whether the inherent immunogenicity of the eCPMV particle in the lung could induce anti-tumour immunity in the B16F10 intravenous model of lung metastatic melanoma. Indeed, weekly intratracheal injection of 100μg of eCPMV (Fig. 3a) resulted in significantly reduced tumour burden as assessed by both metastatic-like tumour foci number (Fig. 3b,c) and tyrosinase expression (Fig. 3d). Tyrosinase-related protein 1 (Tyrp1) is a melanocyte-specific gene[24] whose expression in the lung is restricted to B16F10 tumour cells, which provides a different, more quantitative measure of tumour development and serves as a control for the varying sizes of metastatic-like foci.

Anti-tumour efficacy is immune-mediated and broadly applicable

We determined whether the immune system was required for treatment efficacy by repeating our experimental design described in Figure 3 in the following transgenic mice: Il-$12^{-/-}$, Ifn-$\gamma^{-/-}$, and NOD/scid/IL2R$\gamma^{-/-}$. We did not observe a significant difference in lung tumour burden between eCPMV- and PBS-treated mice in the absence of Il-12 (Fig. 4a), Ifn-γ (Fig. 4b), or in NOD/scid/Il2R$\gamma^{-/-}$(NSG) mice lacking T, B, and NK cells (Fig. 4c).

eCPMV accumulates in and activates neutrophils in the lungs of B16F10 tumour-bearing mice (Fig. 2a–c). Additionally, we detected significant increases in neutrophil-associated cytokines and chemokines in the mouse lung following eCPMV inhalation (Fig. 2d). Therefore, we depleted neutrophils using an anti-Ly6G monoclonal antibody to assess the necessity of neutrophils for treatment efficacy. Depletion of neutrophils from tumour-bearing mice abrogated the anti-tumour effect that we observed in WT mice (Fig. 4d). This, combined with the lack of efficacy observed in Il-12$^{-/-}$, Ifn-$\gamma^{-/-}$, and NSG mice leads us to conclude that the anti-tumour effect of eCPMV inhalation on B16F10 development is through immunomodulation of the lung tumour microenvironment and, in contrast to most tumour immunotherapies, requires neutrophils.

We sought to ascertain whether eCPMV treatment efficacy was restricted to the B16F10 metastatic lung model or if the immunomodulatory anti-tumour effect could transfer to other models. To study treatment of truly metastatic disease in the lung, we utilised the 4T1 BALB/c syngeneic breast cancer model, a transferrable yet genuinely metastatic model. 4T1 tumours established in the mammary fat pad spontaneously metastasise to the lung by day 16, at which point we surgically removed the primary tumour and began eCPMV treatment, injecting intratracheally to affect lung tumour development. The 4T1 cells also expressed luciferase, allowing us to track metastatic lung tumour development. Mice treated intratracheally with eCPMV particles had significantly delayed lung tumour onset and significantly extended survival (Fig. 5a). Mice from eCPMV and PBS treatment groups had comparable primary mammary fat pad tumour burden at day of surgical removal (Supplementary Fig. 5). Therefore, differences in tumour development and survival were due to treatment. No mice from either group experienced recurrence of primary mammary fat pad tumours.

To determine whether the eCPMV particle's unambiguous efficacy in both the B16F10 and 4T1 metastatic lung models was unique to the lung immune environment, we also tested its ability to treat dermal tumours. Intradermal CT26 tumour colon growth was significantly delayed following direct injection with eCPMV (Fig. 5b) and treated tumours rapidly developed necrotic centres.

We also investigated the therapeutic effect of eCPMV in a model of disseminated peritoneal serous ovarian carcinoma[25]. ID8-*Defb29/Vegf-A*-challenged mice treated weekly with eCPMV exhibited significantly improved survival relative to PBS-treated controls (Fig. 5c).

eCPMV immunotherapy induces systemic anti-tumour immunity

Finally, we tested the efficacy of eCPMV in treating dermal B16F10 melanomas. Direct injection of eCPMV resulted in the rapid formation of necrotic centres within the tumours (Fig. 6a) and, in half of the eCPMV-treated mice, resulted in elimination of the tumours altogether after only two treatments (Fig. 6b, 6c). eCPMV intratumoural injection was superior to direct injection with other profoundly immunogenic compounds including LPS, poly(I:C), and the STING agonist DMXAA, none of which induced complete or durable tumour regression (Supplementary Fig. 6). We also tested whether *in situ* vaccination with the eCPMV particles had induced systemic anti-tumour immunity against B16F10 tumours.

Surviving mice (Fig. 6c) were re-challenged with B16F10 on their contralateral flanks 4 weeks after complete disappearance of their primary tumours was confirmed. Mice previously cured of primary B16F10 flank tumours by intratumoural injection of eCPMV exhibited resistance to secondary re-challenge (Fig. 6d), with 3 of 4 re-challenged mice completely rejecting the re-challenge. This indicates that direct injection of primary tumours with eCPMV nanoparticles had induced a protective systemic immune response against B16F10 tumours. It is important to note that the anti-tumour effects of eCPMV in the tested models are not attributable to direct tumour cell cytotoxicity, as exposure to high concentrations of the particle *in vitro* had no effect on cancer cell viability or proliferation (Supplementary Fig. 7). Therefore, we conclude that the striking anti-tumour effect induced by eCPMV nanoparticle treatment is fully immune-mediated and translatable to a variety of tumour models across diverse anatomical sites.

Conclusions

eCPMV nanoparticles are immunotherapeutic to a high degree and clearly modulate the tumour immune environment. There are no previously recognised immunostimulatory reagents in eCPMV. Other self-assembling plant virus-like particles such as Papaya Mosaic Virus nanoparticles have been shown to possess adjuvant-like properties, but these were attributable to ssRNA in the particle, as immunogenicity required TLR7[26]. eCPMV is RNA-free, as determined by extensive characterisation (Supplementary Fig. 8)[17]. Therefore, the immunostimulatory effect is not dependent on TLR stimulation by RNA. Additionally, eCPMV is unlike VLPs that are manufactured in *E. coli* or other microorganisms that may contain immunogenic contaminants. Endotoxin levels measured using a *Limulus* Amebocyte Lysate assay revealed no detectable LPS. We hypothesise that the immunogenicity of eCPMV is attributable to the structure of the VLP. Immunogenicity of the bacteriophage Qβ virus-like particle is related to its particulate nature[27]. The repetitive protein structure of viral capsid nanoparticles may constitute a novel pathogen-associated molecular pattern. We cannot, however, test the immunogenicity of free CPMV single coat proteins as was done with Qβ[27] since isolated S and/or L coat proteins from CPMV virions are insoluble[28]. An alternative would be to test the immunogenicity of VP60, the precursor to the self-assembling mature CPMV coat proteins or identify other VLPs with similar anti-tumour immunogenicity that can be assayed after disassembly

eCPMV inhalation transforms the lung tumour microenvironment and both requires and activates Ly6G+ neutrophils, a population minimally associated with tumour immunotherapy. eCPMV has been shown to bind surface vimentin on cancer cells[29,30] and some antigen-presenting cells[31], although it is not known if murine neutrophils have surface vimentin. eCPMV appears to target quiescent neutrophils and activate them and increases the frequency of $CD11b^{+}$class-$II^{+}CD86^{hi}$ tumour-infiltrating neutrophils. In fact, activated and tumour-infiltrating, or “N1”, neutrophils are the only innate immune cell populations that significantly change following eCPMV lung exposure, both dramatically increasing as a percentage of $CD45^{+}$ cells (from 3% to 21%), and in total number (Fig. 2b). Neutrophils are viewed canonically as sentinels for microbial infection that quickly engulf and kill bacteria before undergoing apoptosis. It appears that neutrophils possess phenotypic plasticity analogous to the M1/M2 polarisation of macrophages[22]. Studies have shown infiltration of

an immunosuppressive, pro-angiogenic “tumour-associated neutrophil” population in B16F10 metastatic lung[32], human liver cancer[33], sarcoma[34], and lung adenocarcinoma[35] that is correlated with enhanced tumour progression. Alternatively, depletion of tumour-resident immunosuppressive neutrophils, conversion of them to a pro-inflammatory phenotype, or recruitment of activated neutrophils into the tumour microenvironment is associated with therapeutic efficacy[22]. Activated neutrophils can directly kill tumour cells via release of reactive oxygen intermediates[23], but can also prime $CD4^+$ T cells and polarise them to a Th1 phenotype[36,37], cross-prime $CD8^+$ T cells[38], and modulate NK cell function[23]. Activated neutrophils can produce Cxcr3 ligands Cxcl9 and Cxcl10 that recruit $CD4^+$ and $CD8^+$ T cells[39] that are correlated with anti-tumour immunotherapeutic efficacy in melanoma models[40,41]. Our data showing increased immunostimulatory neutrophil populations (Fig. 2b) correlates with our cytokine data (Fig. 2d) of increases in neutrophil chemoattractants as well as cytokines and chemokines produced by neutrophils. This data also correlates with our *in vivo* tumour progression data showing that neutrophils are required for eCPMV anti-tumour efficacy.

Interestingly, although many cytokine and chemokine levels were elevated to a statistically significant degree following eCPMV treatment, changes were modest when compared to the dramatic differences in actual tumour burden (Fig. 3b–d). Moreover, we did not observe large increases in pro-inflammatory cytokines Tnf-α or Il-6 that are known to cause lung tissue damage[42]. It appears that eCPMV treatment of lung tumours is effective without eliciting the inflammatory cytokines that cause acute lung injury. This assertion is further supported by histology showing lack of injury or inflammation in lung tissue or other major organs in eCPMV-treated animals (Supplementary Fig. 4). Slight thickening of the alveolar wall, observed in both eCPMV and PBS groups, was likely caused by the intratracheal injection itself rather than eCPMV-treatment.

eCPMV inhalation exhibited efficacy as a monotherapy (Fig. 3) that is very clearly immune-mediated (Fig. 4). This is novel because the eCPMV particle does not directly kill tumour cells (Supplementary Fig. 7) or share any antigenic overlap with B16F10 tumours, but induces an anti-tumour response that requires Th1-associated cytokines Il-12 (Fig. 4a) and Ifn-γ (Fig. 4b), adaptive immunity (Fig. 4c), and neutrophils (Fig. 4d). This suggests that the inherent immunogenicity of the eCPMV nanoparticle, when introduced into the lung, disrupts the tolerogenic nature of the tumour microenvironment, either facilitating a pre-existing anti-tumour immune response, or stimulating a *de novo* anti-tumour response, or both.

This work also shows that eCPMV anti-tumour efficacy in the intravenous B16F10 metastatic lung model is not an artifact of the C57BL6 mouse strain or the B16F10 model, as eCPMV therapy works impressively in ovarian carcinoma and two BALB/c models of metastatic breast and colon cancer (Fig. 5). Constitutive luciferase expression in 4T1 breast carcinoma cells and intradermal challenges of B16F10 and CT26 allowed us to measure tumour progression in real time in a manner not feasible in the B16F10 lung model. We observed a potent and rapid anti-tumour effect that significantly delayed tumour progression and, in the intradermal tumours, induced rapid involution of established tumours and formation of necrotic centres (Fig. 5b and Fig. 6a). Such early responses to eCPMV—3 days

post-intratumoural injection—suggest that eCPMV particles are inducing innate immune cell-mediated anti-tumour responses.

While we are cautious about quantitatively comparing treatments conducted in different labs, it is worth noting that eCPMV appears particularly potent in treating ovarian cancer. Mice receiving eCPMV in the ID8-*Defb29/Vegf-A* ovarian model survive longer in comparison to mice treated with other reported immunotherapies in this model including live, attenuated *Listeria monocytogenes* strain[43], avirulent *Toxoplasma gondii*[44], combination agonistic CD40 and poly(I:C)[45], or Il-10 blocking antibody[46]. Direct injection of B16F10 dermal melanoma tumours with eCPMV induced complete regression of tumours in half of the treated mice and, in these mice that cleared primary tumours, resulted in systemic protective anti-tumour immunity. These observations suggest T-cell mediated immune memory against tumour antigens. eCPMV treatment was superior in direct comparison to high dose LPS, poly(I:C), and STING agonist (Supplementary Fig. 6).

We present here the first report of a VLP-based nanoparticle utilised directly as a cancer immunotherapy agent rather than delivery platform and, furthermore, an immunotherapy that specifically targets and activates neutrophils within the tumour microenvironment to coordinate downstream anti-tumour immune responses. The eCPMV nanoparticle, alone, is immunogenic and highly effective as a monotherapy. However, it can also serve as a nanocarrier for tumour antigens, drugs, or immune adjuvants, opening up the exciting possibility that eCPMV can be modified to deliver a payload that further augments and improves its immunotherapeutic efficacy.

The eCPMV nanoparticle is an effective immunotherapy against tumours originating from a variety of organs. Efficacious does of eCPMV are well-tolerated with no observable toxic side-effects. In summary, the eCPMV self-assembling VLP is an exciting new platform for the treatment of cancer that exerts its therapeutic efficacy through unleashing the power of anti-tumour immunity.

Methods

eCPMV Production and Characterisation

eCPMV capsids were produced through agroinfiltration of *Nicotiana benthamiana* plants with a culture of *Agrobacterium tumefaciens* LBA4404 transformed with the binary plasmid pEAQexpress-VP60-24K, which contains genes for the coat protein precursor VP60 and its 24K viral proteinase to cleave it into its mature form. Six days post infiltration, the leaves were harvested and eCPMV extracted using established procedures (51). PVPP was added during purification to remove plant phenolics. Dye-labeled formulations were made by reacting eCPMV with Alexa Fluor 488 maleimide at 2mg/mL concentration with 10% (v/v) DMSO in 0.1M potassium phosphate buffer then purifying by ultracentrifugation pelleting. The particle concentration was measured using UV/Vis spectroscopy (ε280nm = 1.28$mg^{-1}mLcm^{-1}$), and particle integrity was determined by transmission electron microscopy, fast protein liquid chromatography, and agarose gel electrophoresis. Capsid proteins were further analysed by SDS-PAGE and Western blotting. Quantification of LPS in the sample was measured using an LAL Chromogenic Endotoxin Quantitation Kit (Pierce)

and revealed LPS levels below the detectable level of 50pg/50μg of eCPMV. Full characterisation of eCPMV particles is available in Supplementary Fig. 8.

Mice

C57BL/6J (01C55) females were purchased from the National Cancer Institute or The Jackson Laboratory. Il-12p35−/− (002692), Ifn-γ−/− (002287), BALB/c (000651), and NOD/scid/Il2Rγ−/− (005557) female mice were purchased from The Jackson Laboratory. Mice used in experiments were 8–10 weeks of age. All mouse studies were performed in accordance with the Institutional Animal Care and Use Committee of Dartmouth.

Tumour Models

The B16F10 murine melanoma cell line was obtained from Dr. David Mullins (Geisel School of Medicine at Dartmouth College, Hanover, New Hampshire). 4T1-luciferase murine mammary carcinoma cells were provided by Ashutosh Chilkoti (Duke University, Durham, NC). B16F10, 4T1-luc, and CT26 were cultured in complete media (RPMI supplemented with 10% FBS and penicillin/streptomycin). ID8-*Defb29/Vegf-A* orthotopic ovarian serous carcinoma cells were cultured in complete media supplemented with sodium-pyruvate (52) as previously described. Cells were harvested, washed in phosphate-buffered saline (PBS), and injected in the following manner depending on tumour model: 1.25×10^5 live cells injected intravenously in 200μL PBS in the tail vein (B16F10 metastatic lung), 1.25×10^5 live cells injected intradermally in 30μL PBS in the right flank (B16F10 flank), 1×10^5 live cells injected intradermally in 30μL PBS in the right flank (CT26 flank), 2×10^6 live cells injected intraperitoneally in 200μL PBS (ID8-*Defb29/Vegf-A* peritoneal ovarian). Surviving mice from B16F10 flank direct injections were re-challenged per the same protocol on the contralateral flank 4 weeks following disappearance of primary tumours. For 4T1-luc tumour challenge, 1×10^5 live cells were injected in 30μL of PBS into the left mammary fat pad on day 0 and the tumour was surgically removed on day 16, a day by which it is well-established that the tumour has spontaneously metastasised to the lung (53). Complete removal of primary 4T1-luc tumours was confirmed by bioluminescent imaging. B16F10 and ID8-*Defb29/Vegf-A* are syngeneic for the C57BL6J strain, whereas CT26 and 4T1-luc are syngeneic for the BALB/c background. In regards to authentication of the cell lines, none of the cell lines used in this publication are listed in the Database of Cross-Contaminated or Misidentified Cell Lines of ICLAC. All cell lines have been tested for mycoplasma contamination and found free of mycoplasma prior to freezing and then thawed and used experimentally.

eCPMV Treatment Scheduling

WT, Il-12−/−, Ifn-γ−/−, NOD/scid/IL2Rγ−/−, and Ly6G-depleted mice challenged intravenously with B16F10 were intubated and intratracheally injected with 100μg of eCPMV in 50μL PBS on days 3, 10, and 17 post-tumour challenge. For lung challenge experiments, mice were euthanised on day 21 for quantification of metastatic-like lesions and tyrosinase expression. 4T1-luc-bearing mice were intratracheally injected with 20μg of eCPMV in 50μL PBS on day 16 (same day as primary tumour removal) and again on day 23 (day 7 post-tumour removal). CT26 flank tumours were intratumourally injected with 100μg eCPMV on day 8 post-tumour challenge once they had reached 10mm2 and again on day 15.

Flank tumour diameters were measured every other day and mice were euthanised when tumour diameters reached 200mm2. ID8-*Defb29/Vegf-A* mice were injected IP with 100μg of eCPMV weekly beginning on day 7 post-tumour challenge and euthanised when they reached 35g due to ascites development. B16F10 flank tumours were intratumourally injected with 100μg eCPMV on day 7 post-tumour challenge once tumours had reached 10mm2 and again on day 14. No animals enrolled in experiments were excluded during analysis. Tumour-challenged animals were randomised to treatment groups prior to commencement of treatment but were not blided for assessing outcome and data analysis.

Antibodies and Flow Cytometry

Anti-mouse antibodies were specific for CD45 (30-F11), MHC-II (M5/114.15.2), CD86 (GL-1), CD11b (M1/70), F4/80 (BM8), and Ly6G (1A8) from Biolegend and CD16/CD32 (93) from eBioscience. WT and B16F10 lung tumour-bearing mice were intratracheally injected with 100μg Alexa-488-labeled CPMV particles 24hr prior to euthanisation. Lungs were harvested and dissociated into single cell suspension using the Miltenyi mouse lung dissociation kit (cat# 130-095-927). Red blood cells were removed using lysis buffer of 150mM NH4Cl, 10mM KHCO3, and 0.5mM EDTA. Flow cytometry was performed on a MACSQuant analyzer (Miltenyi). Data were analysed using FlowJo software version 8.7.

Tyrosinase mRNA Expression Analysis

Whole lungs were dissociated and total RNA was extracted using the RNeasy kit (Qiagen, 74104). cDNA was synthesised using iScriptTM cDNA synthesis kit (Bio-Rad, 170-8891). q-PCR was performed on a CFX96TM Real-Time PCR Detection System (Bio-Rad) using iQTM SYBR® Green Supermix (Bio-Rad, 170-8882) with primers at a concentration of 0.5μM. Tyrp1 primer sequences are as follows: forward 5′-ACTTGATGGGATCCAGAAGC-3′, reverse 5′-CTGATTGGTCCACCCTCAGT-3′. mRNA transcript fold-change was calculated using the ΔCT method with all samples normalised to mouse Gapdh.

Cytokine Assay

For *in vivo* cytokine data, total lung homogenate was harvested from B16F10 lung tumour-bearing mice 24hr post-inhalation of 100μg eCPMV particles, which was day 8 post-tumour challenge. For *in vitro* cytokine results, bone marrow-derived dendritic cells (BMDCs) and thioglycollate-stimulated peritoneal macrophages, both derived from C57BL6 mice, were cultured at 1×10^6 cells/well in 200μL complete media in 96-well round-bottomed plates with either 20μg of eCPMV or PBS. Supernatant was harvested after 24hr incubation. Cytokines were quantified using mouse 32plex Luminex assay (MPXMCYTO70KPMX32, Millipore).

Cell Depletion

Mice were injected with mAb depleting Ly6G (clone 1A8) that was purchased from Bio-X-Cell (cat# BE0075-1) and administered IP in doses of 500μg one day prior to eCPMV treatment and then once weekly for the duration of survival experiments. Greater than 95% depletion of target cell populations in the lung was confirmed by flow cytometry (Supplementary Fig. 9).

IVIS Imaging

Mice were injected IP with 150mg/kg of firefly D-luciferin in PBS (PerkinElmer cat#122799) and allowed to rest for 10min. Imagining was conducted using the Xenogen VivoVision IVIS Bioluminescent and Fluorescent Imager platform and analysed with Living Image 4.3.1 software (PerkinElmer).

Statistics

Unless noted otherwise, all experiments were repeated at least 2 times with 4–12 biological replicates to enable statistical analysis and results were similar between repeats. Replicates were kept to between 4–12 due to cost considerations for *in vivo* work. Figures denote statistical significance of $p < 0.05$ as *, $p < 0.01$ as **, and $p < 0.001$ as ***. A p-value < 0.05 was considered to be statistically significant. Data for bar graphs was calculated using unpaired Student's t-test. Error bars represent standard error of the mean from independent samples assayed within the represented experiments. Flank tumour growth curves were analysed using two-way ANOVA. Survival experiments utilised the log-rank Mantel-Cox test for survival analysis. Statistical analysis was done with GraphPad Prism 4 software.

Supplementary Material

Refer to Web version on PubMed Central for supplementary material.

Acknowledgments

We thank the following for their assistance: Zachary Parker; the lab of David Mullins; the lab of Brent Berwin; the Immune Monitoring Lab and DartLab at the Geisel School of Medicine at Dartmouth, particularly Gary Ward and John DeLong; the Dartmouth Transgenic and Genetic shared resource; the Dartmouth Hitchcock Medical Center pathology department; the Irradiation, Pre-clinical Imaging, and Microscopy (IPIM) and Genomics/Molecular Biology (GMB) shared resources at the Norris Cotton Cancer Center. Shared resources at Dartmouth are made possible through generous Centers of Biomedical Research Excellence support. Work was supported by Dartmouth Immunobiology of Myeloid and Lymphoid Cells National Institutes of Health Training Grant 5T32AI007363–22 (P.H.L.), Case Western Reserve University Cardiovascular Research National Institutes of Health Training Grant T32 HL105338 (A.M.W.), National Science Foundation CMMI 1333651 (N.F.S.), Dartmouth Center of Nanotechnology Excellence NIH 1 U54 CA151662 (S.F.), Center for Molecular, Cellular, and Translational Immunological Research NIGMS 1P30RR032136–01 (S.F.), and Norris Cotton Cancer Center P30 CA023108-27 (S.F.).

References

1. Pardoll DM. The blockade of immune checkpoints in cancer immunotherapy. Nat Rev Cancer. 2012; 12:252–264. [PubMed: 22437870]
2. Kershaw MH, Westwood JA, Darcy PK. Gene-engineered T cells for cancer therapy. Nat Rev Cancer. 2013; 13:525–541. [PubMed: 23880905]
3. Ali OA, et al. Identification of immune factors regulating antitumor immunity using polymeric vaccines with multiple adjuvants. Cancer Res. 2014; 74:1670–1681. [PubMed: 24480625]
4. Callahan MK, Postow MA, Wolchok JD. CTLA-4 and PD-1 Pathway Blockade: Combinations in the Clinic. Front Oncol. 2015; 4
5. Winograd R, et al. Induction of T cell immunity overcomes complete resistance to PD-1 and CTLA-4 blockade and improves survival in pancreatic carcinoma. Cancer Immunol Res. 2015; canimm.0215.2014. doi: 10.1158/2326-6066.CIR-14-0215
6. Robert C, et al. Ipilimumab plus dacarbazine for previously untreated metastatic melanoma. N Engl J Med. 2011; 364:2517–2526. [PubMed: 21639810]

7. Andtbacka RHI, et al. Talimogene Laherparepvec Improves Durable Response Rate in Patients With Advanced Melanoma. J Clin Oncol. 2015; JCO.2014.58.3377. doi: 10.1200/JCO.2014.58.3377
8. Corrales L, et al. Direct Activation of STING in the Tumor Microenvironment Leads to Potent and Systemic Tumor Regression and Immunity. Cell Rep. 2015; 11:1018–1030. [PubMed: 25959818]
9. Sheen MR, Lizotte PH, Toraya-Brown S, Fiering S. Stimulating antitumor immunity with nanoparticles. Wiley Interdiscip Rev Nanomed Nanobiotechnol. 2014; 6:496–505. [PubMed: 25069691]
10. Halperin SA, et al. Comparison of safety and immunogenicity of two doses of investigational hepatitis B virus surface antigen co-administered with an immunostimulatory phosphorothioate oligodeoxyribonucleotide and three doses of a licensed hepatitis B vaccine in healthy adults 18–55 years of age. Vaccine. 2012; 30:2556–2563. [PubMed: 22326642]
11. Huber B, et al. A Chimeric 18L1-45RG1 Virus-Like Particle Vaccine Cross-Protects against Oncogenic Alpha-7 Human Papillomavirus Types. PLoS ONE. 2015; 10:e0120152. [PubMed: 25790098]
12. Rynda-Apple A, Patterson DP, Douglas T. Virus-like particles as antigenic nanomaterials for inducing protective immune responses in the lung. Nanomed. 2014; 9:1857–1868.
13. Rynda-Apple A, et al. Virus-Like Particle-Induced Protection Against MRSA Pneumonia Is Dependent on IL-13 and Enhancement of Phagocyte Function. Am J Pathol. 2012; 181:196–210. [PubMed: 22642909]
14. Wiley JA, et al. Inducible Bronchus-Associated Lymphoid Tissue Elicited by a Protein Cage Nanoparticle Enhances Protection in Mice against Diverse Respiratory Viruses. PLoS ONE. 2009; 4:e7142. [PubMed: 19774076]
15. Patterson DP, Rynda-Apple A, Harmsen AL, Harmsen AG, Douglas T. Biomimetic Antigenic Nanoparticles Elicit Controlled Protective Immune Response to Influenza. ACS Nano. 2013; 7:3036–3044. [PubMed: 23540530]
16. Richert LE, et al. CD11c+ cells primed with unrelated antigens facilitate an accelerated immune response to influenza virus in mice. Eur J Immunol. 2014; 44:397–408. [PubMed: 24222381]
17. Saunders K, Sainsbury F, Lomonossoff GP. Efficient generation of cowpea mosaicvirus empty virus-like particles by the proteolytic processing of precursors in insect cells and plants. Virology. 2009; 393:329–337. [PubMed: 19733890]
18. Aljabali AAA, Shukla S, Lomonossoff GP, Steinmetz NF, Evans DJ. CPMV-DOX Delivers. Mol Pharm. 2013; 10:3–10. [PubMed: 22827473]
19. Yildiz I, Lee KL, Chen K, Shukla S, Steinmetz NF. Infusion of imaging and therapeutic molecules into the plant virus-based carrier cowpea mosaic virus: Cargo-loading and delivery. J Controlled Release. 2013; 172:568–578.
20. Costantini C, et al. Neutrophil activation and survival are modulated by interaction with NK cells. Int Immunol. 2010; 22:827–838. [PubMed: 20739460]
21. Gabrilovich DI, Ostrand-Rosenberg S, Bronte V. Coordinated regulation of myeloid cells by tumours. Nat Rev Immunol. 2012; 12:253–268. [PubMed: 22437938]
22. Fridlender ZG, et al. Polarization of Tumor-Associated Neutrophil (TAN) Phenotype by TGF-β: ‘N1’ versus ‘N2’ TAN. Cancer Cell. 2009; 16:183–194. [PubMed: 19732719]
23. Mantovani A, Cassatella MA, Costantini C, Jaillon S. Neutrophils in the activation and regulation of innate and adaptive immunity. Nat Rev Immunol. 2011; 11:519–531. [PubMed: 21785456]
24. Zhu ML, Nagavalli A, Su MA. Aire Deficiency Promotes TRP-1–Specific Immune Rejection of Melanoma. Cancer Res. 2013; 73:2104–2116. [PubMed: 23370329]
25. Conejo-Garcia JR, et al. Tumor-infiltrating dendritic cell precursors recruited by a β-defensin contribute to vasculogenesis under the influence of Vegf-A. Nat Med. 2004; 10:950–958. [PubMed: 15334073]
26. Lebel M-È, et al. Nanoparticle Adjuvant Sensing by TLR7 Enhances CD8+ T Cell–Mediated Protection from Listeria Monocytogenes Infection. J Immunol. 2014; 192:1071–1078. [PubMed: 24376264]
27. Link A, et al. Innate immunity mediates follicular transport of particulate but not soluble protein antigen. J Immunol Baltim Md 1950. 2012; 188:3724–3733.

28. Wu GJ, Bruening G. Two proteins from cowpea mosaic virus. Virology. 1971; 46:596–612. [PubMed: 5137799]
29. Steinmetz NF, Cho CF, Ablack A, Lewis JD, Manchester M. Cowpea mosaic virus nanoparticles target surface vimentin on cancer cells. Nanomed. 2011; 6:351–364.
30. Satelli A, Li S. Vimentin in cancer and its potential as a molecular target for cancer therapy. Cell Mol Life Sci. 2011; 68:3033–3046. [PubMed: 21637948]
31. Gonzalez MJ, Plummer EM, Rae CS, Manchester M. Interaction of Cowpea Mosaic Virus (CPMV) Nanoparticles with Antigen Presenting Cells In Vitro and In Vivo. PLoS ONE. 2009; 4:e7981. [PubMed: 19956734]
32. Jablonska J, Leschner S, Westphal K, Lienenklaus S, Weiss S. Neutrophils responsive to endogenous IFN-β regulate tumor angiogenesis and growth in a mouse tumor model. J Clin Invest. 2010; 120:1151–1164. [PubMed: 20237412]
33. Kuang DM, et al. Peritumoral neutrophils link inflammatory response to disease progression by fostering angiogenesis in hepatocellular carcinoma. J Hepatol. 2011; 54:948–955. [PubMed: 21145847]
34. Pekarek LA, Starr BA, Toledano AY, Schreiber H. Inhibition of tumor growth by elimination of granulocytes. J Exp Med. 1995; 181:435–440. [PubMed: 7807024]
35. Wislez M, et al. Hepatocyte Growth Factor Production by Neutrophils Infiltrating Bronchioloalveolar Subtype Pulmonary Adenocarcinoma Role in Tumor Progression and Death. Cancer Res. 2003; 63:1405–1412. [PubMed: 12649206]
36. Abdallah DSA, Egan CE, Butcher BA, Denkers EY. Mouse neutrophils are professional antigen-presenting cells programmed to instruct Th1 and Th17 T-cell differentiation. Int Immunol. 2011; 23:317–326. [PubMed: 21422151]
37. van Gisbergen KPJM, Sanchez-Hernandez M, Geijtenbeek TBH, van Kooyk Y. Neutrophils mediate immune modulation of dendritic cells through glycosylation-dependent interactions between Mac-1 and DC-SIGN. J Exp Med. 2005; 201:1281–1292. [PubMed: 15837813]
38. Beauvillain C, et al. Neutrophils efficiently cross-prime naive T cells in vivo. Blood. 2007; 110:2965–2973. [PubMed: 17562875]
39. Pelletier M, et al. Evidence for a cross-talk between human neutrophils and Th17 cells. Blood. 2010; 115:335–343. [PubMed: 19890092]
40. Clancy-Thompson E, et al. Peptide Vaccination in Montanide Adjuvant Induces and GM-CSF Increases CXCR3 and Cutaneous Lymphocyte Antigen Expression by Tumor Antigen–Specific CD8 T Cells. Cancer Immunol Res. 2013; 1:332–339. [PubMed: 24377099]
41. Baird JR, et al. Immune-Mediated Regression of Established B16F10 Melanoma by Intratumoral Injection of Attenuated Toxoplasma gondii Protects against Rechallenge. J Immunol. 2013; 190:469–478. [PubMed: 23225891]
42. Caramori G, Adcock IM, Di Stefano A, Chung KF. Cytokine inhibition in the treatment of COPD. Int J Chron Obstruct Pulmon Dis. 2014; 9:397–412. [PubMed: 24812504]
43. Lizotte PH, et al. Attenuated Listeria monocytogenes reprograms M2-polarized tumor-associated macrophages in ovarian cancer leading to iNOS-mediated tumor cell lysis. Oncoimmunology. 2014:3.
44. Baird JR, et al. Avirulent Toxoplasma gondii Generates Therapeutic Antitumor Immunity by Reversing Immunosuppression in the Ovarian Cancer Microenvironment. Cancer Res. 2013; 73:3842–3851. [PubMed: 23704211]
45. Scarlett UK, et al. In situ Stimulation of CD40 and Toll-like Receptor 3 Transforms Ovarian Cancer–Infiltrating Dendritic Cells from Immunosuppressive to Immunostimulatory Cells. Cancer Res. 2009; 69:7329–7337. [PubMed: 19738057]
46. Hart K, Byrne K, Molloy M, Usherwood E, Berwin B. IL-10 immunomodulation of myeloid cells regulates a murine model of ovarian cancer. T Cell Biol. 2011; 2:29.
51. Sainsbury F, Saxena P, Aljabali AAA, Saunders K, Evans DJ, Lomonossoff GP. Genetic engineering and characterisation of Cowpea mosaic virus empty virus-like particles. Methods Mol Biol Clifton NJ. 2014; 1108:139–53.
52. Lizotte, PH.; Baird, JR.; Stevens, CA.; Lauer, P.; Green, WR.; Brockstedt, DG., et al. Attenuated Listeria monocytogenes reprograms M2-polarized tumour-associated macrophages in ovarian

cancer leading to iNOS-mediated tumour cell lysis. Oncoimmunology [Internet]. 2014 May 23. [cited 2015 Feb 27];3. Available from: http://www.ncbi.nlm.nih.gov/pmc/articles/PMC4106169/

53. Pulaski, BA.; Ostrand-Rosenberg, S. Current Protocols in Immunology [Internet]. John Wiley & Sons, Inc; 2001. Mouse 4T1 Breast Tumour Model. [cited 2015 Mar 13]. Available from: http://onlinelibrary.wiley.com/doi/10.1002/0471142735.im2002s39/abstract

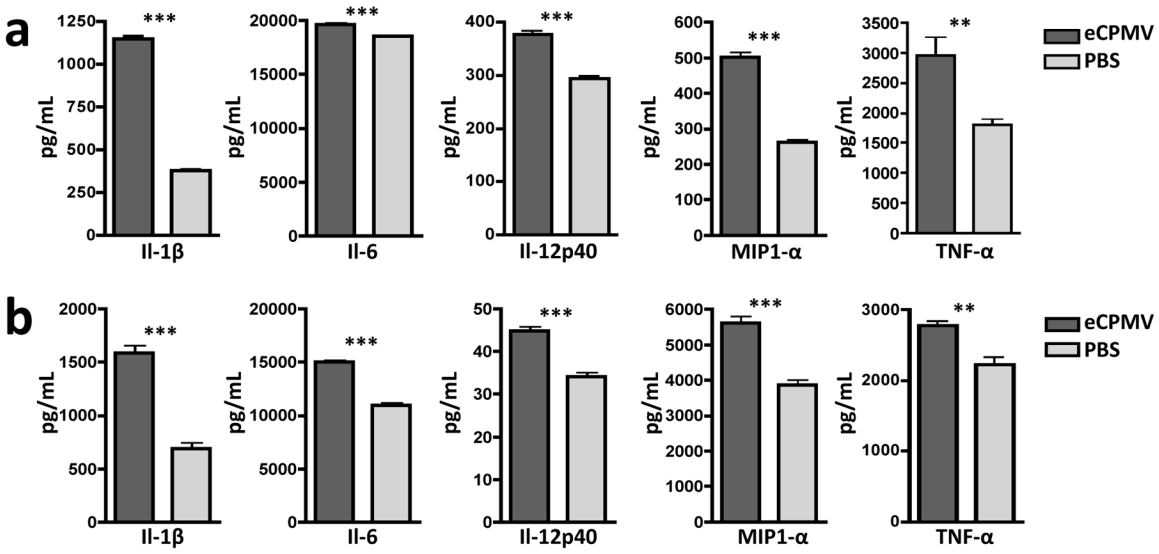

Figure 1. eCPMV nanoparticles are inherently immuonogenic

a, Bone marrow-derived dendritic cells (BMDCs) exposed to eCPMV produce elevated levels of pro-inflammatory cytokines *in vitro*. **b**, Thioglycollate-elicited primary macrophages also secrete significantly elevated levels of the same panel of cytokines. Both cell types (n = 6/group) were cultured for 24hr with 20μg eCPMV (dark gray bars) and cytokine levels were analysed using a multiplexed luminex array. Data for bar graphs calculated using unpaired Student's *t*-test with $p < 0.05$ as *, $p < 0.01$ as **, and $p < 0.001$ as ***.

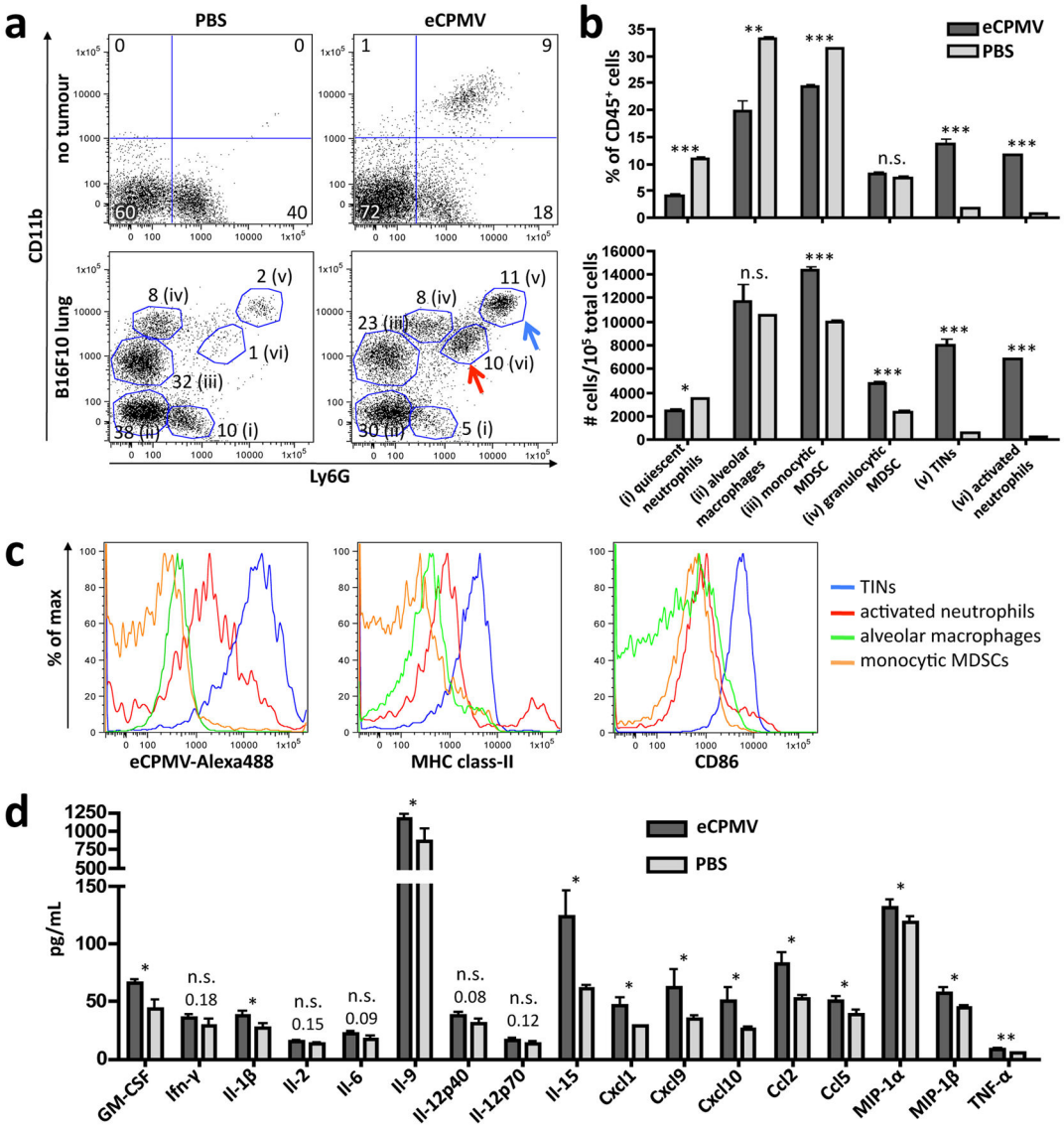

Figure 2. eCPMV inhalation induces dramatic changes in lung immune cell composition and cytokine/chemokine milieu in mice bearing B16F10 lung tumours

a, Representative FACS plots pre-gated on live CD45$^+$ cells of non-tumour-bearing mice treated with PBS (top left) or eCPMV (top right) and B16F10 lung tumour-bearing mice treated with PBS (bottom left) or eCPMV (bottom right). B16F10 mice were treated on day 7 post-B16F10 IV injection. Lungs were harvested 24hr after intratracheal injection of PBS or 100ug eCPMV. Labeling indicates (i) quiescent neutrophils, (ii) alveolar macrophages, (iii) monocytic MDSCs, (iv) granulocytic MDSCs, (v) tumour-infiltrating neutrophils, and (vi) activated neutrophils. Numbers beside circled groups are % of CD45$^+$ cells. Arrows indicate TINs (blue) and CD11b$^+$ activated neutrophils (red). Gating strategies available in Supplemental Fig. 3. **b**, Changes in innate cell subsets induced by eCPMV inhalation in tumour-bearing mice (n = 5/group) are quantified as a percentage of CD45$^+$ cells (top) and total number of cells (bottom) as presented in panel **a. c**, Representative histograms for TINs (blue), activated neutrophils (red), alveolar macrophages (green), and monocytic MDSCs

(orange) indicating mean fluorescence intensity (MFI) uptake of Alexa488-labeled CPMV, class-II, and CD86 activation markers. **d**, Lungs of B16F10 lung tumour-bearing mice (n = 5/group) exhibited elevated levels of pro-inflammatory cytokines and chemoattractants when treated with eCPMV as in panel **a**. Data for bar graphs calculated using unpaired Student's *t*-test with $p < 0.05$ as *, $p < 0.01$ as **, and $p < 0.001$ as ***.

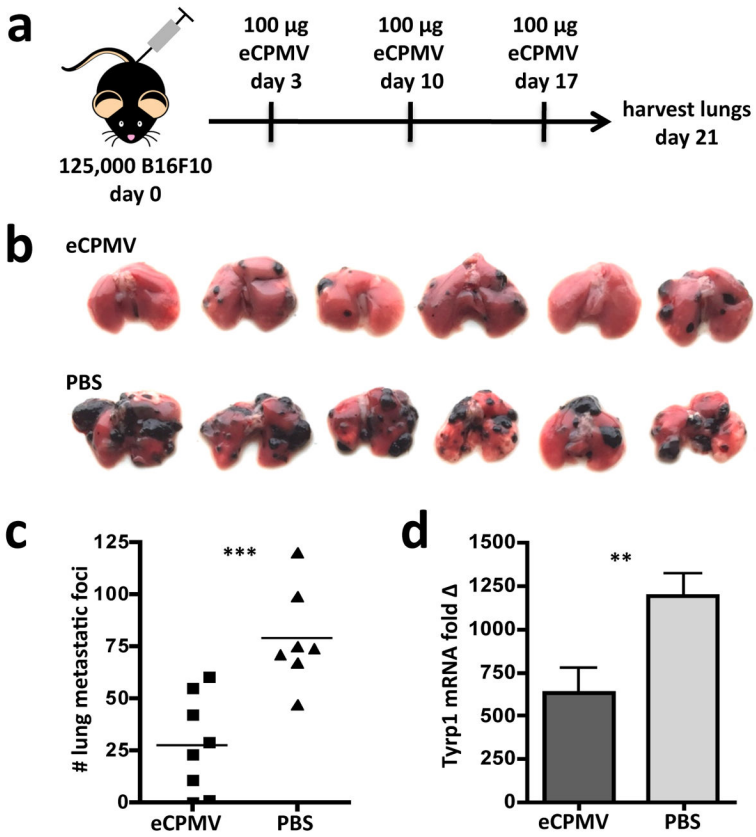

Figure 3. eCPMV inhalation reduces formation of B16F10 metastatic-like lung tumours

a, Schematic of experimental design. **b**, Photographic images of lungs from eCPMV- and PBS-treated B16F10 tumour-bearing mice on day 21 post-tumour challenge. **c–d,** B16F10 lung metastatic-like tumour foci were quantified both by number in **c** or by qRT-PCR assay for melanocyte-specific Tyrp1 mRNA expression in **d** (n = 8 eCPMV, 7 PBS). Data for bar graphs calculated using unpaired Student's *t*-test with $p < 0.05$ as *, $p < 0.01$ as **, and $p < 0.001$ as ***.

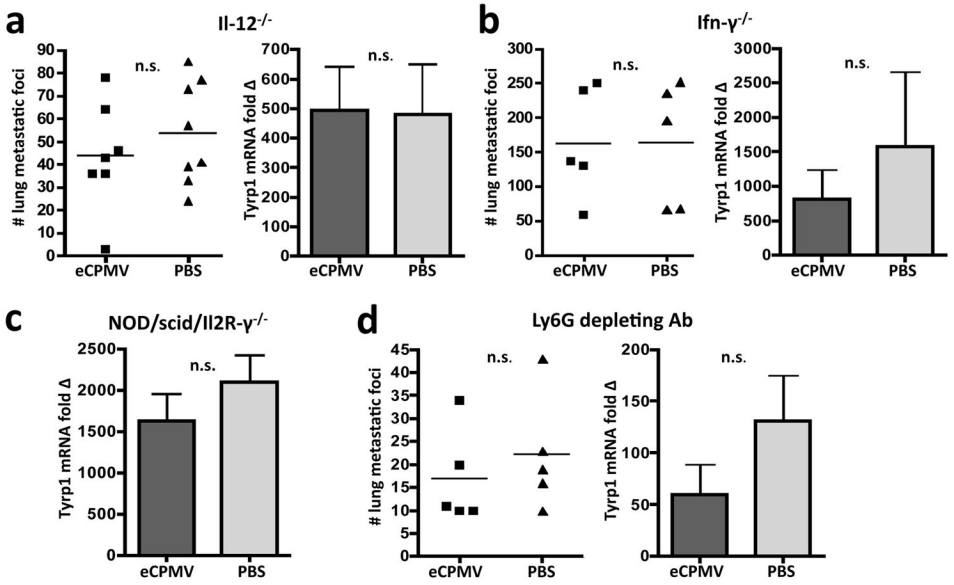

Figure 4. eCPMV treatment efficacy in B16F10 lung model is immune-mediated

a, eCPMV inhalation did not significantly affect tumour progression when mice lack Il-12 (n = 7 eCPMV, 8 PBS). **b**, Treatment efficacy was also abrogated in the absence of Ifn-γ (n = 5/group). **c**, NOD/scid/Il2R-$\gamma^{-/-}$ mice lacking T, B, and NK cells also failed to respond to eCPMV inhalation therapy (n = 5/group). **d**, Depletion of neutrophils with Ly6G mAb abrogates treatment efficacy (n = 5/group). Data for bar graphs calculated using unpaired Student's *t*-test with $p < 0.05$ as *, $p < 0.01$ as **, and $p < 0.001$ as ***.

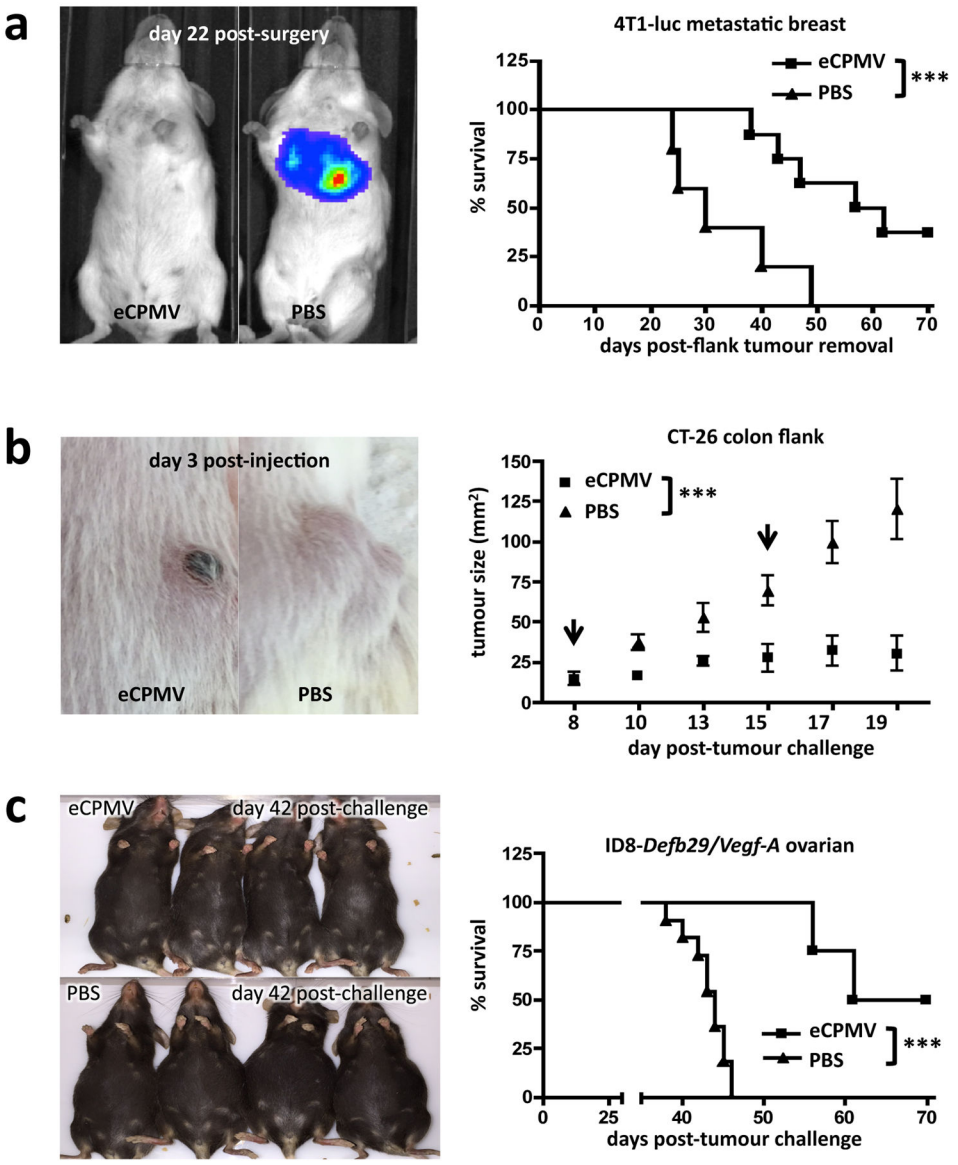

Figure 5. eCPMV immunotherapy is successful in metastatic breast, colon, and ovarian carcinoma models

a, Mice challenged with 4T1 breast tumours and intratracheally injected with PBS rapidly developed (IVIS images) and succumbed (Kaplan-Meier) to metastatic lung tumours beginning on day 24 post-surgical removal of primary tumour, whereas tumour development was delayed and survival significantly extended in mice receiving intratracheal injection of eCPMV (n = 8 eCPMV, 5 PBS). **b**, Mice bearing intradermal flank CT26 colon tumours also responded to direct injection of eCPMV (arrows indicate treatment days) with significantly delayed growth when compared to PBS-injected controls (n = 5/group). **c**, eCPMV also proved successful as a therapy for ID8-*Defb29*/*Vegf-A* ovarian cancer-challenged mice, significantly improving survival when injected IP relative to PBS-injected controls (n = 4 eCPMV, 11 PBS). eCPMV-treated mice displayed no visible ascites on day 42 post-challenge while PBS-treated controls had reached endstage criteria. Survival experiments

utilised the log-rank Mantel-Cox test for survival analysis and flank tumour growth curves were analysed using two-way ANOVA, with $p < 0.05$ as *, $p < 0.01$ as **, and $p < 0.001$ as ***.

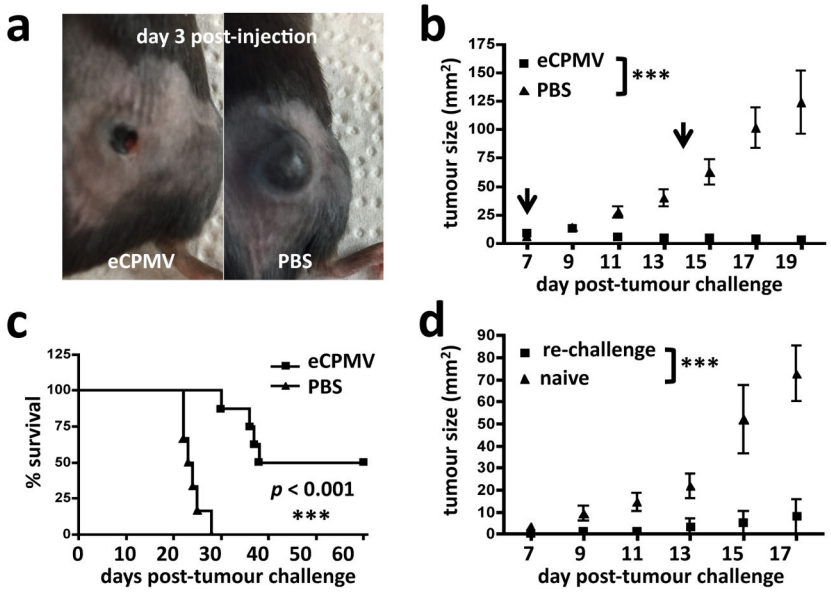

Figure 6. eCPMV induces systemic, durable anti-tumour immunity

a–b, Mice bearing intradermal flank B16F10 tumours directly injected with eCPMV (arrows indicate treatment days) showed noticeably delayed tumour progression relative to PBS-injected controls (n = 8 eCPMV, 6 PBS). **c**, Half of eCPMV-treated mice experienced complete elimination of primary tumours (n = 8 eCPMV, 6 PBS). **d**, The majority of mice cured of primary tumours by eCPMV treatment and re-challenged on the opposite flank 4 weeks later failed to develop new tumours (n = 4/group). Survival experiments utilised the log-rank Mantel-Cox test for survival analysis and flank tumour growth curves were analysed using two-way ANOVA, with $p < 0.05$ as *, $p < 0.01$ as **, and $p < 0.001$ as ***.